FULL PAPER DOI: 10.1002/adsc.201800561

Advanced Synthesis & Catalysis

Very Important Publication

Heteroatom Donor-Decorated Polymer-Immobilized Ionic Liquid Stabilized Palladium Nanoparticles: Efficient Catalysts for Room-Temperature Suzuki-Miyaura Cross-Coupling in Aqueous Media

Simon Doherty,[a,*] Julian G. Knight,[a,*] Tom Backhouse,[a] Einas Abood,[a] Hind Al-shaikh,[a] Ashley R. Clemmet,[a] Jack R. Ellison,[a] Richard A. Bourne,[b] Thomas W. Chamberlain,[b] Rebecca Stones,[b] Nicholas J. Warren,[b] Ian J. S. Fairlamb,[c] and Kevin R. J. Lovelock[d]

[a] NUCAT, School of Chemistry, Bedson Building, Newcastle University, Newcastle upon Tyne, NE1 7RU, UK
Tel: +44 (0) 191 208 6537
Fax +44 (0) 191 208 6929
E-mail: simon.doherty@ncl.ac.uk; j.g.knight@ncl.ac.uk
[b] Institute of Process Research & Development, School of Chemistry and School of Chemical and Process Engineering, University of Leeds, Woodhouse Lane, Leeds LS2 9JT, UK
[c] Department of Chemistry, University of York, Heslington, York YO10 5DD, UK
[d] School of Chemistry, Food and Pharmacy, University of Reading, Reading, RG6 6AT, UK

Received: May 1, 2018; Revised: July 12, 2018; Published online: August 3, 2018

Supporting information for this article is available on the WWW under https://doi.org/10.1002/adsc.201800561

Abstract: Palladium nanoparticles stabilized by heteroatom donor-modified polystyrene-based polymer immobilized ionic liquids (PdNP@HAD-PIILP; HAD-PPh_2, OMe, NH_2, CN, pyrrolidone) are highly efficient catalysts for the Suzuki-Miyaura cross-coupling in aqueous media under mild conditions. Catalyst modified with phosphine was consistently the most efficient as it gave high yields across a range of substrates under mild conditions at low catalyst loadings. Incorporation of polyethylene glycol into the phosphine modified immobilised ionic liquid support improved catalyst efficacy by improving dispersibility and facilitating access to the active site. Moreover, each of the heteroatom modified catalysts was more active than the corresponding unsubstituted imidazolium-based polystyrene benchmark as well as commercial samples of Pd/C. Catalyst generated *in situ* from either $[PdCl_4]$@PPh_2-PIILP or its PEGylated counterpart $[PdCl_4]$@PPh_2-PEGPIILP, by reduction with phenylboronic acid, outperformed their pre-formed counterparts for the vast majority of substrates examined. The turnover frequency of 16,300 h^{-1} obtained at room temperature is one of the highest to be reported for palladium nanoparticle-catalysed Suzuki-Miyaura cross-coupling between 4-bromoacetophenone and phenylboronic acid in aqueous media under such mild conditions.

Keywords: Palladium nanoparticles; immobilised ionic liquids; heteroatom donor; stabilisation; Suzuki-Miyaura cross-coupling; aqueous media

Introduction

Transition metal-catalysed aryl-aryl and aryl-heteroaryl bond formation is a powerful tool in synthesis as the resulting biaryls are key motifs in a host of important bioactive natural products, pharmaceutical intermediates, fine chemicals and functional materials.[1] While high activities have been achieved for the coupling of aryl chlorides with aryl boronic acids using homogeneous palladium catalysts based on sterically demanding electron-rich phosphines such as Buchwald's biaryl monophosphines,[2] Beller's *cataCXium*,[3] Stradiotto's Dalphos,[4] the Doherty-Knight KITPHOS monophosphines[5] and Kwong's indolyl-based monophosphines,[6] these systems suffer numerous drawbacks including the use of expensive oxygen sensitive phosphines, organic solvents, contamination of the product with palladium and difficulty recovering the catalyst for purification and recycling. To this end, transition metal nanoparticles are evolving into a highly versatile class of catalyst for the Suzuki-Miyaura cross-coupling,[7] in addition to a host of

other useful organic transformations.[8] The high activity associated with these nanoparticles has been attributed to the number of catalytically active atoms per unit area of the surface i.e. the high surface to volume ratio and quantum confinement effects.[9] However, the high surface energy of small nanoparticles drives their aggregation towards larger species which are less active and/or selective.[10] One solution to this problem has been to impregnate the nanoparticles into supports such as mesoporous silicas,[11] metal oxides,[12] zeolites,[13] porous carbon structures,[14] metal organic frameworks[15] and polymers[16] to provide steric stabilization. More recently, ionic liquids have been shown to act as both solvent and stabilizer for a host of transition metal nanoparticles and the ability to modify and tailor their physicochemical properties and functionality offers immense potential for developing new catalyst technology.[17] Unfortunately, the use of ionic liquids also suffers several practical limitations including high cost compared with water or a traditional solvent, high viscosity and leaching of the ionic liquid during work-up or continuous flow operation.[18] In addition, while the primary stabilisation of nanoparticles by ionic liquids is believed to result from weak electrostatic interactions that are easily displaced to allow access to the active site,[19] they do not always provide sufficient stabilization against aggregation under working conditions. This problem has been addressed by incorporating a metal-binding heteroatom donor such as an amine,[20] phosphine,[21] nitrile,[22] thiol,[23] hydroxyl[24] and bipyridine[25] into the ionic liquid on the basis that the additional covalent interactions would improve the long term stability of the nanoparticles as well as control the kinetics of formation.[26] Indeed, this strategy has proven successful and there have been reports of marked improvements in catalyst performance including; (i) enhancements in activity and selectivity for hydrogenations catalysed by PdNPs stabilised with either ionophilic phosphine-based ligands[27a,b] or 2,2′-dipyridylamine-functionalised ionic liquids,[27c] (ii) improved recyclability for NiNPs stabilised by an amino-modified imidazolium-based ionic liquid[28a] and (iii) switchable chemoselectivity for the hydrogenation of aryl ketones and aldehydes catalysed by RuNPs stabilised with phosphine-functionalised ionic liquids.[29] However, the large volumes often required, their high cost and the difficulty associated with recovering and purifying the ionic liquid after catalysis are major issues that severely limit their implementation.

Polymer Immobilized Ionic Liquids (PIILs)[30] are an emerging class of functional material that combine the favourable properties of a polymer support with the well-documented advantages of an ionic liquid environment such as catalyst stabilization, facile catalyst activation, ease of recycling and enhancements in rate and selectivity.[31] Moreover, covalent attachment of an ionic liquid to a polymer has several additional benefits as it prevents leaching of the ionic liquid, improves durability, facilitates separation and recovery of the catalyst and reduces the volume of ionic liquid required to a single or double layer rather than bulk solvent; this could ultimately result in a significant cost saving. We have recently initiated a program to develop heteroatom donor-decorated polymer immobilised ionic liquids with the intention of combining the stabilization provided by a heteroatom donor and an ionic liquid with a polymer support to explore whether the nature of the heteroatom donor and its loading influences nanoparticle formation, specifically their size, morphology and efficacy as catalysts.[32] Moreover, there may well be additional benefits associated with incorporating heteroatom donors into polymer immobilised ionic liquids that could result from modifying the surface electronic structure, the hydrophilicity and/or steric properties of the ligand as well as the ionic microenvironment. For example, RuNP stabilised by amino-modified alumina (RuNP-NH_2-γ-Al_2O_3) are markedly more efficient catalysts for the hydrogenation of levulinic acid than Ru/γ-Al_2O_3; this was attributed to the highly dispersed electron rich ruthenium centres[33] and ultra-small PtNPs stabilised by triphenylphosphine-modified silica are significantly more chemoselective for the catalytic hydrogenation of acetophenone and styrene than its unmodified counterpart, the NPs of which are much larger.[34] In other recent examples, phosphorus donors have been shown to control the size, shape and electronic properties of rhodium, ruthenium and gold nanoparticles and thereby their performance as selective catalysts for the hydrogenation of arenes and α,β-unsaturated aldehydes,[35] and surface modification by *N*-heterocyclic carbenes has been shown to; (i) influence the performance and stability of ruthenium and palladium nanoparticles as catalysts for oxidations and reductions,[36] (ii) activate unreactive Pd/Al_2O_3 for the Buchwald-Hartwig amination[37] and (iii) tune reactivity and selectivity of Ru/K-Al_2O_3 for chemoselective hydrogenation.[38]

Interested in exploring the influence of the number and type of heteroatom donors on the formation and efficacy of polymer immobilised ionic liquid-stabilised palladium nanoparticles, we have undertaken a comparison of the efficiency of palladium nanoparticles stabilised by various heteroatom donor-modified polymer immobilised ionic liquids as catalyst for the Suzuki-Miyaura cross-coupling (Figure 1). While initially cautious that the use of the large excess of capping agent required to maximize surface coverage might restrict or block access to the active site,[39] a handful of recent studies provide convincing evidence that such a strategy could actually improve catalyst

performance.[40] For example, Yuan and co-workers demonstrated that the combination of a polymer immobilized ionic liquid and a polytriazolium-derived poly(*N*-heterocyclic carbene) act synergistically to stabilize a range of metal nanoparticles with precisely controlled sizes of 1 nm and a record high catalytic performance for rhodium-catalysed methanolysis of ammonia borane was reported,[40a] while Huang obtained a marked enhancement in selectivity for the liquid phase aerobic oxidation of benzyl alcohol catalysed by silica supported Au nanoparticles capped with chemisorbed polyvinylpyrrolidone.[40b] Herein, we describe the results of this comparison which has shown that (i) PdNPs stabilised by heteroatom donor-modified polymer immobilised ionic liquids outperform their unmodified counterpart, (ii) catalyst stabilised by phosphine-based PIIL is more efficient than those stabilized by other heteroatom donors such as nitrile, methoxy, amide, and hydroxyl, (iii) catalyst stabilised by PEGylated phosphine-decorated polymer immobilised ionic liquid consistently outperformed its non-PEGylated counterpart and, moreover, is among the most active PdNP-based system to be reported for Suzuki-Miyaura cross-coupling in aqueous media at room temperature and (iv) catalysts generated *in situ* by reduction of tetrachloropalladate-loaded polymer immobilised ionic liquid ($PdCl_4$@HAD-PIIL) are typically more efficient than their preformed counterparts (PdNP@HAD-PIIL) across the majority of substrates examined.

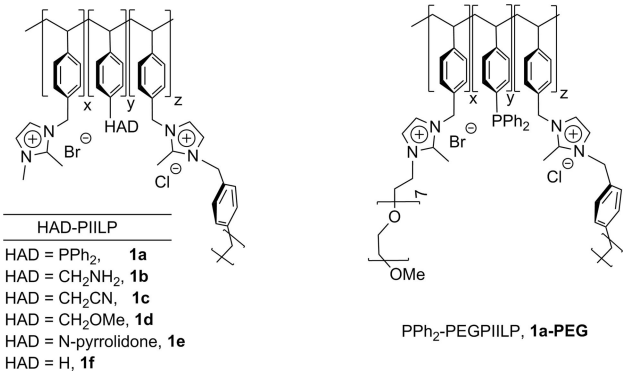

Figure 1. Composition of polymer immobilised ionic liquids **1a–f** and **1a-PEG** used in this study.

Results and Discussion

Heteroatom donor-decorated polymers **1a–f** were prepared by AIBN-initiated radical polymerisation of imidazolium-modified styrene monomer, heteroatom donor modified styrene and dicationic cross-linker in a 1.86:1:0.14 ratio (Scheme 1). The ratio of heteroatom donor-based monomer to imidazolium co-monomer/cross-linker was chosen such that complete exchange of bromide for tetrachloropalladate would correspond to a heteroatom donor to palladium ratio of one. Polymers **1a–f** were impregnated with tetrachloropalladate by ion exchange in water to afford $PdCl_4$@HAD-PIILP (**2a–f**) as brown-red solids in near quantitative yield. The corresponding PIIL-stabilised nanoparticles PdNP@HAD-PIILP (**3a–f**) were prepared by sodium borohydride reduction of **2a–f** in ethanol and isolated as black powders in high yield (Scheme 1).

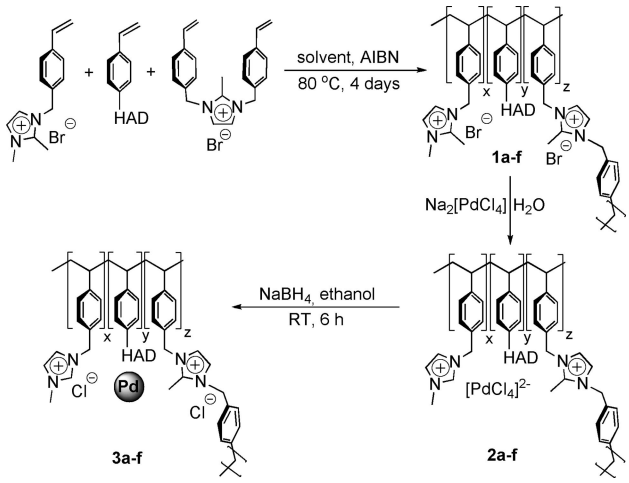

Scheme 1. Synthesis of polymers **1a–f**, $[PdCl_4]^{2-}$ impregnated polymers **2a–f** and PIILP-stabilized palladium nanoparticles **3a–f**.

Polymers were typically characterised by solution NMR spectroscopy, TGA, SEM and IR spectroscopy while palladium-loaded systems were characterised using a combination of solid state NMR spectroscopy, IR, XPS, TEM, SEM and ICP-OES; full details are provided in the ESI. The thermal stability of polymers **1a–f** was investigated by thermogravimetric analysis and differential scanning calorimetry. The TGA profiles of **1a–f** showed an initial weight loss just below 100 °C due to removal of physisorbed water and ethanol; this was followed by two or three main degradation pathways between 240–300 °C confirming that these polymers are entirely suitable for use as supports to stabilise metal nanoparticles for use in catalysis. The palladium loadings of **2a–f** and **3a–f** were determined to be 0.15–2.1 mmol g^{-1} and 0.14–3.0 mmol g^{-1}, respectively, using ICP-OES. The ^{13}C CP/MAS NMR spectra of **1a–f** and **2a–f** contain characteristic signals between δ 120–145 ppm attributed to the imidazolium ring and the aromatic carbon atoms as well as an additional signal at higher field which corresponds to the methyl group on the imidazolium ring. Additional polymer specific signals associated with the heteroatom donor were also

evident and appear at δ75 and 59 ppm (CH_2OMe), δ 24 ppm (CH_2CN), δ176 ppm (C=O, pyrrolidone) and δ49 ppm (CH_2NH_2). Surface characterization of the tetrachloropalladate-loaded precursors **2a–f** was undertaken by X-ray photoelectron spectroscopy (XPS) and a single Pd $3d_{3/2}$ and Pd $3d_{5/2}$ doublet with binding energies of 337.0–337.8 eV and 342.2–343.2 eV is attributed to the Pd^{2+} ion. The X-ray photoelectron spectra of **3a–f** typically contained two pairs of $3d_{3/2}$ and Pd $3d_{5/2}$ doublets; peaks with binding energies of 335.0–335.5 eV and 340.1–340.7 eV correspond to Pd(0) while those with binding energies of 336.1–338.1 eV and 341.2–343.3 eV correspond to surface Pd^{2+} ions (see ESI). Scanning electron microscopy revealed a stark difference in surface morphology of the polymer after exchange of the chloride with palladate (see ESI) as the surface of **1a–f** has a rough granular texture compared with the smoother flat surfaces of **2a–f**. Powder X-ray diffraction data was also collected on **3a–f** to examine/confirm the crystal phase and to compare the mean size of PdNPs determined using the Debye-Scherrer formula with the sizes obtained from analysis of the TEM micrographs. The XRD patterns for **3a**, **3c**, **3d** and **3f** each contained diffraction peaks at 2θ = 40.1, 46.3, 68.5, 82.1 and 86.0 which index to the (111), (200), (220), (311) and (222) lattice planes of the face centered cubic phase of palladium (JCPDS No. 46-1043), consistent with reported literature.[41] In comparison, no diffraction peaks for metallic palladium were detected for **3a-PEG**, **3b** or **3e** which suggests that the palladium particles are highly dispersed with sizes <2.5 nm.[42] TEM micrographs of catalysts **3a–f** revealed that the palladium nanoparticles were near monodisperse with heteroatom-dependent average diameters ranging from 1.7±0.78 to 3.20±0.62 nm, details of which are presented in Table S2; representative micrographs and associated distribution histograms for **3a** and **3a-PEG** based on >100 particles are shown in Figure 2 and those for **3b–f** are presented in the ESI (see ESI).

Interestingly, the disparate sizes of the nanoparticles in **3a–f** may be due to the influence of the heteroatom donor on nucleation and growth of the palladium nanoparticles as the heteroatom to palladium ratio in each of the catalysts is the same by virtue of the 1 to 2 ratio of monomers. To this end, there have been a number of reports providing definitive evidence that the nature of heteroatom can influence nanoparticle size. For example, Rossi obtained smaller palladium nanoparticles in the presence of a phosphine-functionalized support (2.9±0.6 nm) compared with the corresponding amine-modified system (3.8±1.2 nm).[43a,b] More recently, Yang prepared platinum NPs stabilized on triphenylphosphine-modified silica that were smaller than those on unmodified silica and also markedly more chemo-

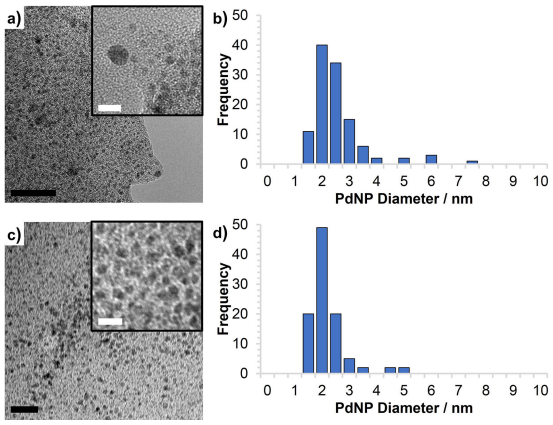

Figure 2. HRTEM images of (a) **3a** and (c) **3a-PEG**, and (b and d) corresponding particle size distributions determined by counting >100 particles. Mean nanoparticle diameters are 2.29±0.96 nm and 1.93±0.67 nm for **3a** and **3a-PEG**, respectively. Black and white scale bars are 25 and 5 nm, respectively. N. B. The size distribution for **3a** has been reported previously in ref 32.

selective for the hydrogenation of acetophenone and phenylacetylene; spectroscopic studies also confirmed the presence of a strong Pt–P interaction between the PPh_3 and PtNPs.[34] The size of palladium nanoparticles stabilized on linker-modified Al-MIL-53 have also been shown to be dependent on the nature of the heteroatom modifier[43c] while the size of ruthenium NPs stabilized by secondary phosphine oxides are substituent dependent.[43d] Stable small and homogenously dispersed ruthenium NPs have been prepared in imidazolium-based ILs in the presence of primary alkyl amines; the mean size of 1.2 nm was independent of the alkyl chain length of the imidazolium ring. In contrast, in the absence of amine the size of the NPs was highly dependent on the length of the alkyl chain; spectroscopic studies provided convincing evidence that the size control was the result of coordination of the amine to the nanoparticle.[43e]

A comparison of the various heteroatom donor-based catalysts **3a–f** was initially undertaken to identify the most efficient system for further optimisation. Preliminary screening focused on the Suzuki-Miyaura cross-coupling between 4-bromoacetophenone and phenylboronic acid as this is the accepted benchmark transformation for catalyst evaluation, full details of which are presented in Table 1. Reactions were initially conducted using 0.05 mol% catalyst in ethanol/water at room temperature and under these conditions high conversions (78–98%) were obtained with **3a–e** after 30 min; for comparison a conversion of only 58% was obtained with the same loading of **3f** which does not contain a stabilising heteroatom donor. As the highest conversion was obtained with catalyst **3a**, the efficacy of its PEGylated **3a-PEG** counterpart

was also examined with the aim of introducing additional weak stabilising interactions and enhancing water compatibility and solubility for use in aqueous phase catalysis.[44] To this end, there are numerous reports of efficient catalysis of the Suzuki-Miyaura cross-coupling with palladium nanoparticles immobilised on PEG-modified stabilisers such as Fe_3O_4@poly (ethylene glycol),[45] tris(triazolyl)-polyethylene glycol,[46] Fe_3O_4@poly(ethylene glycol)-bridged amine-functionalised imidazolium ionic liquids,[47] PEG-substituted phosphine oxides,[48] and PEG-tagged azamacrocycles,[49] PEGylated imidazolium-based phosphinite ionic liquid-modified γ-Fe_2O_3@SiO_2,[50] as well as with size-controlled palladium NPs generated in the presence of varying concentrations of unmodified PEG in water.[51] Gratifyingly, **3a** and its PEGylated counterpart, **3a-PEG**, appear to outperform each of these systems and in most cases under much milder conditions. As complete conversion was also obtained with **3a-PEG** both systems were taken forward for further optimisation and evaluation.

Table 1. Comparison of the palladium-catalysed Suzuki-Miyaura cross-coupling between 4-bromoacetophenone and phenylboronic acid using **3a–f**.[a]

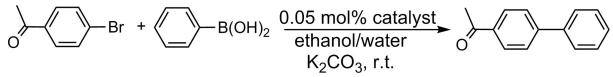

Entry	Catalyst	HAD	Conv (%)[b]	TOF (h^{-1})[c]
1	**3a**	PPh_2	98	3920
2	**3b**	CH_2NH_2	78	3120
3	**3c**	CH_2CN	90	3600
4	**3d**	CH_2OMe	94	3760
5	**3e**	pyrrolidone	94	3760
6	**3f**	H	58	3220
7	**3a-PEG**	PPh_2	100	4000

[a] Reaction conditions: 1.0 mmol 4-bromoacetophenone, 1.13 mmol phenylboronic acid, 1.2 mmol K_2CO_3, 0.05 mol% **3a–f** or **3a-PEG**, 2.4 mL ethanol/water 1/1, room temp., 30 min.

[b] Yields determined by gas chromatography using decane as internal standard. Average of three runs.

[c] Moles of product per mole of catalyst per hour based on total palladium content.

A series of batch reactions with 0.05 mol% of *ex-situ prepared* **3a** or **3a-PEG** explored the effect of solvent and base on catalyst efficacy in order to identify optimum conditions for substrate screening. The results in Table 2 reveal that solvent has a dramatic effect on catalyst efficacy with **3a** and **3a-PEG** both giving high conversions in a water/ethanol mixture (1/1) (entry 7) while reactions conducted in neat ethanol or water (entries 1–2) or conventional organic solvent (entries 3–5) gave much lower conversions. Interestingly, while THF-water has been used the solvent of choice for Suzuki-Miyaura cross-couplings catalysed by homogeneous systems,[52] it gave poor conversions with **3a** and **3a-PEG** (entry 6). As the use of water as an additive/co-solvent to promote the Suzuki-Miyaura cross-coupling is well-documented, a series of reactions were conducted to determine the optimum volumetric ratio of ethanol-water (entries 7–9). While reactions conducted in neat ethanol were slow and only reached 28% conversion after 30 min, addition of water resulted in a dramatic improvement in efficiency such that the optimum volumetric ratio of 1/1 gave complete conversion with no evidence for homocoupling of the aryl bromide (entry 7). This appears to be primarily related to the dispersion of the catalyst in the reaction mixture, with dynamic light scattering (DLS) measurements revealing large aggregates (500 nm to 10 μm) in pure water and ethanol as compared to a clear solution, with ~100 nm particles, observed in a 50:50 water/ethanol mixture (see ESI Figure S66 for full details). The potential green benefits and practical advantages associated with conducting catalysis in aqueous media prompted us to use a 1/1 ethanol-water mixture for the remainder of our studies. While the initial choice of K_2CO_3 as base was guided by literature precedent, a survey of a limited range of alternative bases was undertaken to establish which was the most effective as the correct combination of base and solvent is crucial to achieving good conversions. As expected, high conversions were also obtained with sodium and caesium carbonate as well as potassium phosphate (entries 10–12) while other inorganic bases such as caesium fluoride and alkali-metal acetates (entries 13–15) gave much lower conversions as did tributylamine (entry 16). Finally, the efficiency of **3a** and **3a-PEG** was compared with commercially available samples of 5 mol% Pd/C from various suppliers in order to determine the relative merits of the new catalysts. Three samples were examined and under the same conditions, 0.1 mol% Pd/C catalysed the Suzuki-Miyaura cross-coupling between 4-bromobenzophenone and phenylboronic acid but only reached 9%, 13% and 6% conversion, respectively, in the same time (entries 17–19).

As **3a** and **3a-PEG** are generated from their tetrachloropalladate-based precursors, $PdCl_4$@PPh_2-PIILP (**2a**) and $PdCl_4$@PPh_2-PEGPIILP (**2a-PEG**), respectively, by reduction with sodium borohydride, we examined the possibility of using phenylboronic acid to reduce the precursor *in-situ* immediately prior to addition of substrate. There would be several practical advantages associated with this strategy as it would eliminate the need to prepare, isolate and store the nanoparticle catalysts, and as such it would streamline the protocol, improve versatility by en-

Table 2. Optimization of the Suzuki-Miyaura cross-coupling between 4-bromoacetophenone and phenylboronic acid using **3a** and **3a-PEG**.[a]

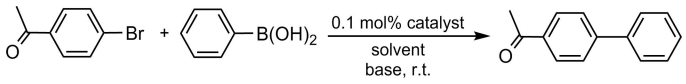

Entry	Catalyst		Solvent	Base	Yield (%)[b]		TOF (h^{-1})[c]	
					3a	**3a-PEG**	**3a**	**3a-PEG**
1	**3a**	**3a-PEG**	ethanol	K_2CO_3	24	28	896	1120
2	**3a**	**3a-PEG**	H_2O	K_2CO_3	10	32	400	1280
3	**3a**	**3a-PEG**	toluene	K_2CO_3	3	3	120	120
4	**3a**	**3a-PEG**	THF	K_2CO_3	2	1	80	40
5	**3a**	**3a-PEG**	DMF	K_2CO_3	12	20	480	800
6	**3a**	**3a-PEG**	THF/H_2O	K_2CO_3	10	15	400	600
7	**3a**	**3a-PEG**	EtOH/H_2O (1/1)	K_2CO_3	98	100	3920	4000
8	**3a**	**3a-PEG**	EtOH/H_2O (3/1)	K_2CO_3	70	66	2800	2640
9	**3a**	**3a-PEG**	EtOH/H_2O (1/3)	K_2CO_3	29	39	1160	1560
10	**3a**	**3a-PEG**	EtOH/H_2O	Na_2CO_3	83	74	3320	2960
11	**3a**	**3a-PEG**	EtOH/H_2O	Cs_2CO_3	91	75	3640	3000
12	**3a**	**3a-PEG**	EtOH/H_2O	K_3PO_4	62	66	2480	2640
13	**3a**	**3a-PEG**	EtOH/H_2O	CsF	22	27	880	1080
14	**3a**	**3a-PEG**	EtOH/H_2O	NaOAc	9	7	360	280
15	**3a**	**3a-PEG**	EtOH/H_2O	CsOAc	11	11	440	440
16	**3a**	**3a-PEG**	EtOH/H_2O	NBu_3	2	5	80	200
17	Pd/C		EtOH/H_2O	K_2CO_3	Pd/C	9	Pd/C	360
18	Pd/C		EtOH/H_2O	K_2CO_3	Pd/C	13	Pd/C	520
19	Pd/C		EtOH/H_2O	K_2CO_3	Pd/C	6	Pd/C	240

[a] Reaction conditions: 1.0 mmol 4-bromoacetophenone, 1.13 mmol phenylboronic acid, 1.2 mmol base, 0.05 mol% **3a–f** and Pd/C, 2.4 mL solvent, room temp., 30 min.
[b] Yields determined by gas chromatography using decane as internal standard. Average of three runs.
[c] Moles of product per mole of catalyst per hour based on total palladium content.

abling different reducing agents and/or conditions to be used where appropriate and facilitate rapid catalyst and reaction screening. To this end, comparative catalyst testing was undertaken by stirring 0.05 mol% **2a** and **2a-PEG** with phenylboronic acid for 10 min immediately prior to addition of 4-bromoacetophenone and under the same conditions the yields of 1-([1,1′-biphenyl]-4-yl)ethan-1-one were comparable to or higher than those obtained with *ex-situ* prepared catalyst; for example, catalyst generated *in-situ* from **2a** and **2a-PEG** gave 96% and 100% conversion, respectively, after only 30 min which matched the conversions obtained with *ex-situ* prepared **3a** and **3a-PEG**. TEM analysis of *in-situ* generated **2a** and **2a-PEG** revealed that the palladium nanoparticles are monodisperse with mean diameters of 2.61 ± 0.38 and 3.36 ± 0.61 nm, respectively (Figure 3); for comparison *ex-situ* prepared **3a** and **3a-PEG** have smaller mean diameters of 2.29 ± 0.96 and 1.93 ± 0.67 nm, respectively.

The robustness of **3a-PEG** was tested by reducing the catalyst loading to 0.001 mol% and under otherwise identical conditions a conversion of 98% was obtained after 6 h; this corresponds to a total turnover number (TON) of 98,000 and an average turnover

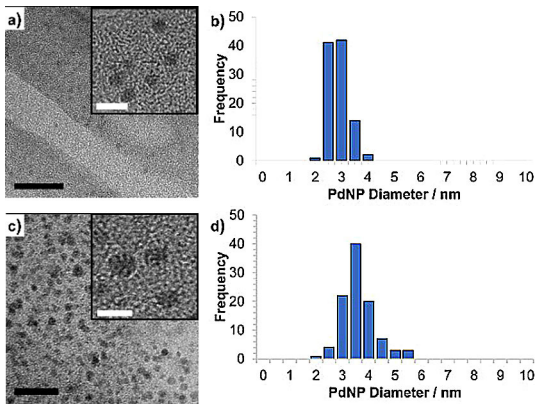

Figure 3. HRTEM images of (a) **3a** and (c) **3a-PEG** generated *in-situ*, and (b and d) corresponding particle size distributions determined by counting >100 particles. Mean nanoparticle diameters are 2.61 ± 0.38 nm and 3.36 ± 0.61 nm for **3a** and **3a-PEG** formed *in-situ*, respectively. Black and white scale bars are 25 and 5 nm, respectively.

frequency (TOF) of 16,300 h^{-1}. Remarkably, **3a-PEG** outperforms tris(triazolyl)-polyethylene glycol stabilised palladium nanoparticles recently developed by Astruc and co-workers which reached a TON 89,000

and a TOF of 2,700 h^{-1} for the Suzuki-Miyaura cross-coupling between bromobenzene and phenyl boronic acid in an ethanol/water mixture;[44] in addition, a significantly higher temperature of 80 °C was required to achieve this efficiency whereas **3a-PEG** operates at room temperature. A survey of the literature revealed that **3a-PEG** also outperforms the vast majority of PdNP-based catalysts for the Suzuki-Miyaura cross-coupling between 4-bromoacetophenone and phenylboronic and is even comparable to water soluble diaminocyclohexane-cyclodextrin-supported PdNPs which gave a TOF of 16,000 h^{-1} based on 32% conversion after 2 h with a catalyst loading of 0.001 mol%.[53] For comparison, the TOF obtained with **3a-PEG** in water/ethanol at room temperature is also a substantial improvement on that of 950 h^{-1} for tris-imidazolium-stabilised PdNPs at 90 °C,[54] 132 h^{-1} for water soluble PdNPs stabilised by PEG-tagged click-derived tris-triazoles at 100 °C,[46] 198 h^{-1} for PdNPs distributed in the framework of ionic liquid-modified ordered mesoporous organosilica at 60 °C,[55] and 310 h^{-1} for magnetically separable Fe_3O_4@PEG-iminophosphine-supported palladium nanoparticles at 65 °C;[45] while each of the above systems required elevated temperatures **3a-PEG** operated efficiently at room temperature. Other PdNP-based systems that catalyse this transformation include supports and stabilisers such as graphene and graphene oxide,[14a] starch,[56] ionic liquid-grafted poly(*p*-phenylene) microspheres,[31d] thiazolidine-based mesoporous silica gel,[57] phosphine-functionalised silica surface,[43a] amino-functionalised metal-organic frameworks,[15g] multi-layered covalently supported ionic liquids,[58] PdNP@benonite,[59] hybrid pyrazoles,[60] and amino-modified silica gel;[11e] however, the TOF obtained in each case was markedly lower than that obtained with **3a-PEG**.

Having identified optimum conditions and obtained an encouraging conversion for the benchmark coupling, catalyst testing was extended to a range of aryl bromides to explore and assess the scope and limitations of these systems. The data in Table 3 compares the performance of catalysts generated *in-situ* from **2a** and **2a-PEG** with their *ex-situ* prepared counterparts **3a** and **3a-PEG** and clearly shows that good conversions can be obtained for the Suzuki-Miyaura cross-coupling of activated and unactivated aryl bromides as well as sterically challenging substrates. Both *ex-situ* prepared catalysts, **3a** and **3a-PEG**, gave high conversions with activated aryl bromides such as 3- and 4-bromobenzonitrile (entry 1–2), 1-bromo-4-nitrobenzene and 1-bromo-3-nitrobenzene (entry 4–5) and 4-bromobenzaldehyde (entry 6), with **3a-PEG** generally outperforming its non-PEGylated counterpart **3a**, albeit by only a small margin in some cases. The cross-coupling between diethyl (2-bromophenyl)phosphonate and phenylboronic acid was also investigated as it is a sterically demanding substrate that would afford a biaryl monophosphonate which could be further elaborated to a biaryl monophosphine; gratifyingly a high conversion was obtained after only 6 h (entry 10). Electron-rich and sterically-demanding coupling partners typically required longer reaction times (5–16 h) to reach comparable conversions at room temperature (entries 3, 7–9 and 11–16), however, reaction times could be reduced quite significantly at elevated temperatures. Inspection of the conversions in Table 3 clearly shows that catalyst generated *in-situ* by reduction of **2a** or **2a-PEG** outperformed their *ex-situ* prepared counterparts across the range of electron-poor and sterically challenging substrates examined; this is most evident for 4-bromoanisole (entries 11), 2-bromoacetophenone (entry 9) and 3-bromotoluene (entry 16). For example, catalyst generated *in-situ* from **2a-PEG** gave 99% conversion for the cross-coupling between 2-bromoacetophenone and phenylboronic acid while its *ex-situ* prepared counterpart **3a-PEG** only reached 91% conversion in the same time; similarly the corresponding non-PEGylated systems **2a** and **3a** reached 58% and 34%, respectively, for the same cross-coupling (entry 9). This comparison also highlights the improvement in performance that can be achieved by attaching a PEG-substituent to the stabilising support as *in-situ* generated and *ex-situ* prepared PdNP@PPh_2-PEGPIILP gave markedly higher conversions than their respective PdNP@PPh_2-PIILP counterparts. Finally, the same protocol was extended to the cross-coupling of 2-bromopyridine and 2-bromopyrimidine (entries 17–18) with phenylboronic acid but, unfortunately, only low yields of the corresponding heterobiaryl were obtained, even after extended reaction times. Thus, it appears that heteroaryl bromides may either deactivate or poison the catalyst through coordination of the nitrogen donor atom to the surface of the nanoparticle as catalyst mixtures containing 0.05 mol% **3a-PEG**, phenylboronic acid and pre-stirred with either 1 mmol of 2-bromopyridine and 2-bromopyrimidine were inactive for the cross-coupling of 4-bromoacetophenone. Even though the phosphines in **3a-PEG** appear to be covalently attached to the surface of the palladium nanoparticles, as evidenced by solid state ^{31}P NMR spectroscopy, the efficacy of this catalyst suggests that either the surface palladium atoms are not all entirely coordinatively saturated or phosphine dissociation is a facile process as the substrate must be able to access the active surface sites. However, the large excess of nitrogen donor-based heteroaromatic substrate may well saturate the surface palladium atoms and deactivate the catalyst. In preliminary work a sample of **3a-PEG** was treated with pyridine to assess the effect of nitrogen donor groups on the activity of the catalyst (see supporting information). A reduction in catalytic

Table 3. Suzuki-Miyaura cross-coupling between phenylboronic acid and a range of aryl bromides catalyzed by *in-situ* generated and *ex-situ* prepared **3a** and **3a-PEG**.[a]

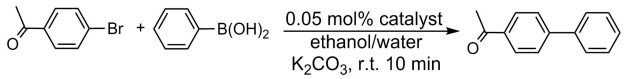

Entry	Ar–Br	Time (h)	Yield (%)[b] (TOF (h^{-1}))[c] **2a**	**2a-PEG**	**3a**	**3a-PEG**
1	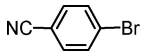	0.5	95 (3800)	99 (3960)	96 (3840)	99 (3960)
2	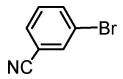	3	80 (534)	99 (660)	96 (640)	99 (660)
3		5	81 (324)	98 (392)	95 (380)	99 (396)
4	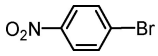	2	89 (890)	91 (910)	96 (960)	98 (980)
5	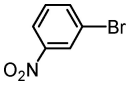	1	96 (1920)	99 (1980)	95 (1900)	99 (1980)
6	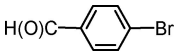	0.5	95 (3800)	97 (3880)	97 (3880)	99 (3960)
7	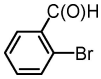	16	93 (116)	98 (122)	83 (104)	92 (116)
8	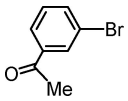	16	95 (120)	99 (124)	81 (102)	99 (120)
9	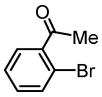	16	58 (82)	99 (124)	34 (42)	91 (114)
10	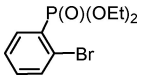	6	89 (296)	99 (330)	57 (190)	92 (306)
11	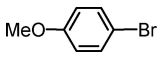	5	62 (248)	97 (388)	45 (180)	93 (372)
12	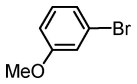	5	31 (124)	89 (356)	31 (124)	96 (384)
13		16	89 (112)	99 (124)	91 (114)	94 (118)
14	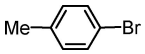	6	96 (320)	90 (300)	85 (284)	89 (296)
15		16	67 (84)	80 (100)	60 (76)	78 (98)
16	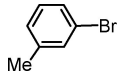	6	80 (266)	49 (164)	87 (290)	69 (230)
17		16	22 (28)	20 (26)	17 (22)	19 (24)
18		16	34 (42)	28 (36)	28 (36)	23 (28)

[a] Reaction conditions: 1.0 mmol aryl bromide, 1.13 mmol phenylboronic acid, 1.2 mmol K_2CO_3, 0.05 mol% catalyst generated *in-situ* from **2a** or **2a-PEG** or *ex-situ* prepared **3a** and **3a-PEG**, 2.4 mL EtOH/H_2O (1/1), room temp, time (h).
[b] Yields determined by gas chromatography using decane as internal standard. Average of three runs.
[c] Moles product per mole catalyst per hour based on total palladium content.

activity was observed after pre-treating **3a-PEG** with 1 mmol of pyridine for either 1 h and 16 h as both gave conversions of only 6% (*c.f.* 100% before addition of pyridine) for the cross-coupling between 4-

bromoacetophenone and phenylboronic acid; this further suggests that coordination of the heteroatom donor to the surface of the nanoparticle may well be responsible for the deactivation/passivation. The variation in conversion as a function of pyridine addition time for the Suzuki-Miyaura cross-coupling between 2-bromotoluene and phenylboronic acid catalysed by 0.1 mol% **3a-PEG** was also monitored by running a series of reactions in parallel, adding 1 mmol of pyridine at different time intervals and working the reaction up after 8 h to obtain conversion as a function of pyridine quenching time. The profile shown in Figure 4 clearly reveals that addition of pyridine results in instantaneous deactivation of the catalyst as the conversions-time profile maps closely to that in Figure 6 for the same reaction conducted in the absence of pyridine (*vide infra*).

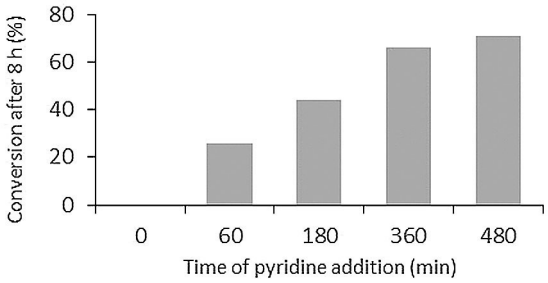

Figure 4. Conversion as a function of pyridine addition time for the Suzuki-Miyaura cross-coupling between 2-bromotoluene and phenylboronic acid, catalysed by 0.1 mol% *ex-situ* prepared **3a-PEG**; each reaction was worked up after 8 h.

Fluorescence-detected X-ray absorption spectroscopy (FD-XAS) of the catalyst after pyridine treatment for 1 h showed an increase in the Pd L_{III} edge energy relative to the untreated **3a-PEG** catalyst of 0.32 ± 0.13 eV which is indicative of a small reduction of the electron density on the palladium metal within the nanoparticles upon pyridine addition (see ESI Figure S67 and Table S3 for full details),[61] However, there is no real change in white line intensity or shape of the edge after addition. Further *in-situ* surface investigations are currently underway to fully elucidate the nature of the coordination environment at palladium in **3a** and **3a-PEG** as well as the influence of added donor atoms under conditions of catalysis.

A preliminary study of the influence on catalyst performance of the surface ionic liquid (IL), diphenylphosphine donor (PPh_2) and PEG has been undertaken by comparing the efficiency of a series of catalysts containing varying combinations of each component.[32] The data summarised in Table 4 demonstrates the marked influence of the phosphino donor on catalyst efficacy as selective removal of this component results in a dramatic drop in TOF from 9840 h^{-1} and 8760 h^{-1} for PdNP@PPh_2-PEGPIILP and PdNP@PPh_2-PIILP to 1560 h^{-1} and 360 h^{-1} for PdNP@PEG-PIILP and PdNP@PIILP, respectively. In addition, selective removal of the ionic liquid also results in a decrease in TOF to 6600 h^{-1} for PdNP@PPh_2-PEGstyrene compared with 9840 h^{-1} for PdNP@PPh_2-PEGPIILP. Although it is clear that each component has a direct effect on catalyst performance, further studies will be required to deconvolute how each component influences catalyst performance, in particular, whether the heteroatom donor influences nanoparticle formation and size and/or surface electronic structure. Moreover, as removal of either the ionic liquid or PEG results in a drop in activity the balance of hydrophilicity/hydrophobicity clearly effects dispersibility and/or swelling and thereby access to the active site.

Interested in exploring the influence of introducing a PEG substituent on the reaction profile, the Suzuki-Miyaura cross-coupling between 4-bromobenzonitrile and phenylboronic acid, catalysed by either 0.1 mol% of *ex-situ* prepared PdNP@PPh_2-PIILP (**3a**) or PdNP@PPh_2-PEGPIILP (**3a-PEG**) was monitored as

Table 4. Suzuki-Miyaura cross-coupling between 4-bromoacetophenone and phenyl boronic acid as a function of catalyst composition.

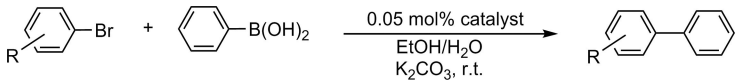

Name	Components present	TOF (h^{-1})
PdNP@PPh_2-PEGPIILP	PPh_2, IL, PEG	9840
PdNP@PPh_2-PIILP	PPh_2, IL	8760
PdNP@PIILP	IL	360
PdNP@PPh_2-styrene	PPh_2	4800
PdNP@PEGPIILP	IL, PEG	1560
PdNP@PPh_2-PEGstyrene	PPh_2, PEG	6600

[a] Reaction conditions: 1.0 mmol 4-bromoacetophenone, 1.13 mmol phenylboronic acid, 1.2 mmol K_2CO_3, 0.05 mol% *ex-situ* prepared catalyst, 2.4 mL EtOH/H_2O (1/1), room temp, time 10 min.

a function of time. The resulting composition-time profile revealed that the latter reaches complete conversion after only 10 min whereas the former requires 15 min to reach completion (Figure 5a–b, ●). Similarly, the corresponding catalyst generated *in situ* from 0.1 mol% $PdCl_4$@PPh_2-PIILP (**2a**) and $PdCl_4$@PPh_2-PEGPIILP (**2a-PEG**) also show qualitatively similar conversion-time profiles (Figures 5a–b, ▲) suggesting that reduction is both facile and does not influence the reaction kinetics. In addition, the data in Figure 5a clearly shows that both PdNP@PPh_2-PIILP systems (i.e. *ex-situ* prepared and *in-situ* generated) experience an induction period of approximately 5 min whereas the PdNP@PPh_2-PEGPIILP system turns over immediately; this may well be due to poorer solvation of **3a** compared with its more hydrophilic PEG-based counterpart. However, the rates of **3a** and **3a-PEG** during the 'active period' appear to be similar.

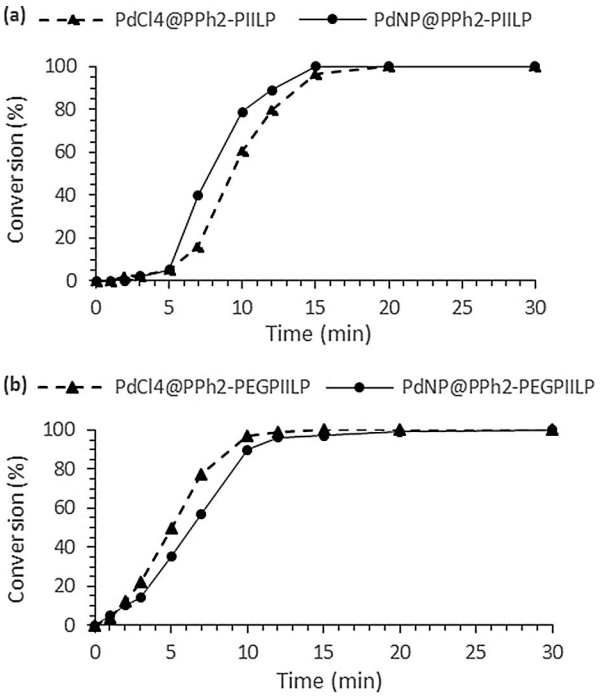

Figure 5. Reaction profile as a function of time for the Suzuki-Miyaura cross-coupling between 4-bromobenzonitrile and phenylboronic acid catalysed by (a) *in-situ* generated (▲) and *ex-situ* prepared (●) **3a** and (b) *in-situ* generated (▲) and *ex-situ* prepared (●) **3a-PEG**.

Although some of the more challenging substrates required long reaction times, the majority reached good conversions within 16 h, with the exception of 2-bromotoluene which only reached 80% and 78% conversion with *in-situ* generated and *ex-situ* prepared **3a-PEG**, respectively. A comparative study of the variation in conversion as a function of time for the Suzuki-Miyaura cross-coupling between 2-bromotoluene and phenylboronic acid catalysed by a 0.1 mol% loading of *in-situ* generated and *ex-situ* prepared **3a-PEG** at room temperature shows that the composition-time profiles are qualitatively similar and that the optimum conversion is essentially reached after 4 h (Figure 6).

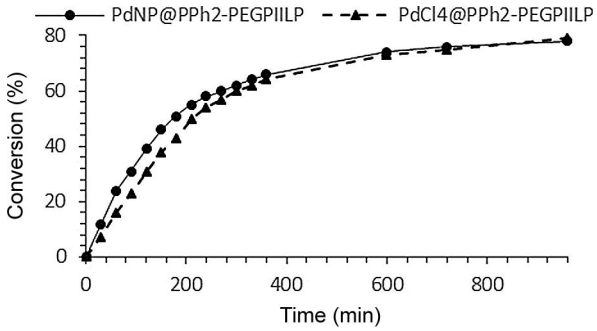

Figure 6. Reaction profile as a function of time for the Suzuki-Miyaura cross-coupling between 2-bromotoluene and phenylboronic acid catalysed by *in-situ* generated (▲) and *ex-situ* prepared (●) **3a-PEG**.

TEM examination of the nanoparticles isolated from the reaction catalysed by *ex situ* prepared PdNP@PPh_2-PEGPIILP revealed that while the palladium nanoparticles remained near monodisperse there has been a significant increase in size with a mean diameter of 3.72 ± 0.58 nm, compared to the sample examined before catalysis which has a mean diameter of 1.93 ± 0.67 nm; the micrograph and associated distribution histogram based on $>$ 100 particles are shown in Figure 7.

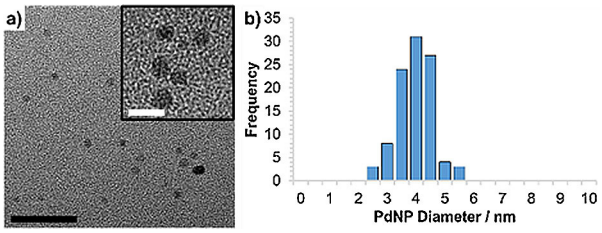

Figure 7. (a) HRTEM image of *ex-situ* prepared PdNP@PPh_2-PEGPIILP (**3a-PEG**) after use in the Suzuki-Miyaura cross-coupling between 2-bromotoluene and phenylboronic acid for 6 h and (b) the corresponding particle size distribution determined by counting $>$100 particles. Mean nanoparticle diameters are 3.72 ± 0.58 nm. Black and white scale bars are 25 and 5 nm, respectively.

The reusability of **3a-PEG** was investigated for the benchmark Suzuki-Miyaura coupling between 4-bromoacetophenone and phenylboronic acid to assess the

robustness and longevity of the catalyst and the potential for incorporation into a flow process. The practical problems associated with recovering the small amount of catalyst (0.05 mol%, 1.0 mg) by filtration prevented us from performing conventional recycle experiments. Instead, reuse experiments were conducted by extracting the product and unreacted starting material with diethyl ether before recharging the aqueous phase with ethanol, 4-bromoacetophenone and phenylboronic acid. A preliminary reuse experiment conducted for 30 min revealed a slight but gradual drop in conversion from 99% to 81% after the 5th run. However, conversions improved when the reaction time was extended to 60 min (Figure 8). Analysis of the organic phase collected after each reuse revealed that the palladium content was too low to be detected by ICP-OES confirming that the drop in activity was not due to leaching of palladium during the extraction. TEM analysis of the aqueous phase remaining after the 5th 60 min run revealed that the palladium nanoparticles were near monodisperse but significantly larger with a mean diameter of 4.9 ± 1.0 nm, compared with 1.93 ± 0.67 nm for freshly prepared catalyst (Figure 9). While this increase in size may account for the drop in activity, we should consider the possibility that conversions may also become mass transfer limited as the reaction mixture becomes progressively more difficult to stir due to the increasing amounts of precipitates that form during reuse. While further studies are clearly required to distinguish between these factors, successful reuse of **3a-PEG** is encouraging and suggests that this system may well be sufficiently robust for use in a scale-up continuous flow process. Interestingly, a reuse experiment for the cross-coupling between 2-bromotoluene and phenylboronic acid catalysed by **3a-PEG** was also conducted and the conversions of 89% and 87% for the first and second runs, respectively, confirmed that the catalyst remained highly active even after 6 h; again this may suggest that the increase in NP size described in Figure 7 does not significantly impact catalyst activity.

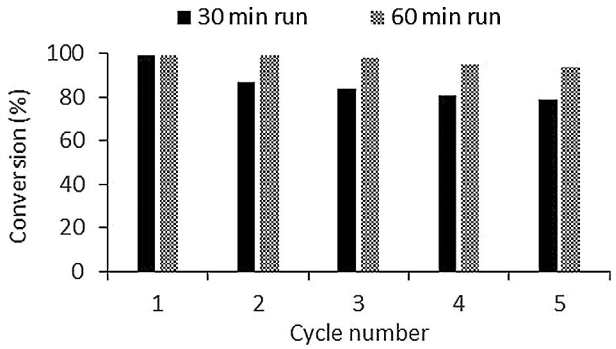

Figure 8. Reuse study for the Suzuki-Miyaura cross-coupling between 4-bromoacetophenone and phenylboronic acid catalysed by *ex-situ* prepared **3a-PEG** for reaction times of 30 min and 60 min.

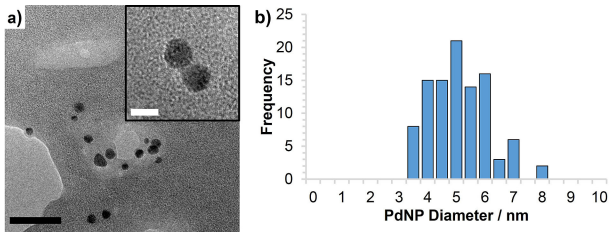

Figure 9. (a) HRTEM image of *ex-situ* prepared PdNP@PPh_2-PEGPIILP (**3a-PEG**) after 5 reuses in the Suzuki-Miyaura cross-coupling between 4-bromoacetophenone and phenyl boronic acid and (b) the corresponding particle size distribution determined by counting >100 particles. Mean nanoparticle diameters are 4.9 ± 1.0 nm. Black and white scale bars are 25 and 5 nm, respectively.

The nature of the active species in palladium nanoparticle-catalysed Suzuki-Miyaura cross-couplings remains controversial due to the difficulty associated with obtaining definitive unambiguous information.[7a,62] While many reports suggest that nanoparticles act as a reservoir that leaches to liberate a soluble active palladium species there is also a significant body of evidence for catalysis at defect sites on the surface of the nanoparticles i.e. a heterogeneous process.[63] Determination of the palladium content remaining in solution after reaction may be misleading as it will not distinguish between a pathway involving leaching and re-deposition (release and capture mechanism). Thus, a series of mercury poisoning tests were conducted for the cross-coupling between 4-bromotoluene and phenylboronic acid using *in-situ* generated and *ex-situ* prepared **3a-PEG** in order to probe the pathway.[62] In these reactions a mixture containing either $PdCl_4$@PPh_2-PEGPIILP (**2a-PEG**) or PdNP@PPh_2-PEGPIILP (**3a-PEG**), phenylboronic acid (to ensure reduction of $[PdCl_4]^{2-}$) and potassium carbonate in water/ethanol was pre-stirred with 400 equivalents of mercury prior to initiating reaction by addition of 4-bromotoluene. A range of pre-stirring times were investigated and the resulting conversion-mercury poisoning time profile (Figure 10) revealed that both catalyst systems experience a marked reduction in conversion from *ca.* 90% in the absence of mercury to 46–50% upon direct addition of mercury with no pre-stirring; conversions continued to drop to 20–22% for 60 min pre-stirring and ultimately to 5% after the pre-stirring was increased to 24 h. Although the drop in activity resulting from the addition of mercury may be taken as evidence for catalysis by surface active palladium,[64] this interpretation must be treated with caution as poisoning is often reported to result in an immediate quench of the reaction. In addition, there have also been a few

reports that mercury can poison molecular Pd(0) species[65] and, thus, gradual deactivation/passivation of the catalyst surface with respect to leaching of active soluble palladium species may also explain the observed conversion-pre-stirring time profile. The gradual drop in conversion as a function of pre-stirring time may well be associated with the efficacy of mixing as the mercury must be well-dispersed in the mixture to poison the catalyst and the use of water/ethanol may limit the efficacy of this process.

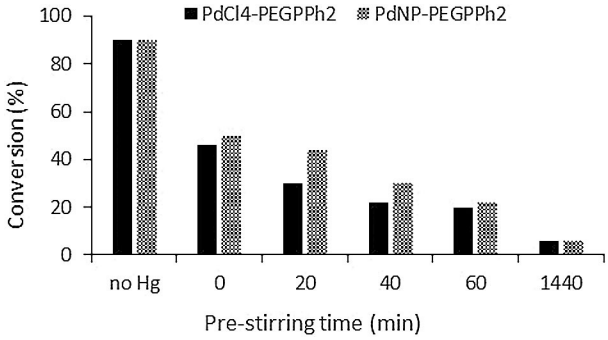

Figure 10. Conversion as a function of Hg(0) pre-stirring time for the Suzuki-Miyaura cross-coupling between 4-bromotoluene and phenylboronic acid catalysed by *in-situ* generated and *ex-situ* prepared **3a-PEG**; all reactions were run for 6 h.

Reaction dilution studies for the cross-coupling between 4-bromotoluene and phenylboronic acid catalysed by *in-situ* generated and *ex-situ* prepared **3a-PEG** under optimum conditions resulted in a slight in increase in conversion as the reaction was diluted from 1.2 mL to 10.0 mL (Figure 11).

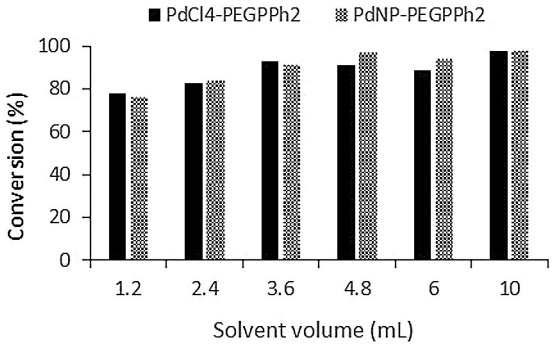

Figure 11. Conversion as a function of reaction volume (dilution) for the Suzuki-Miyaura cross-coupling between 4-bromotoluene and phenylboronic acid catalysed by *in-situ* generated and *ex-situ* prepared **3a-PEG**.

While this is certainly not definitive evidence for catalysis by a heterogeneous system it does eliminate a purely homogeneous pathway. Moreover, at this stage we cannot exclude a pathway involving solubilisation of a surface palladium atom that is captured by a proximal phosphine to afford an active supported mono-coordinate LPd type species (Figure 12).

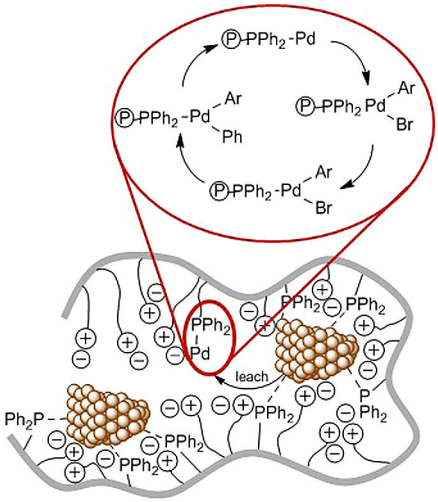

Figure 12. Schematic showing a possible pathway involving capture of leached palladium as an active mono-coordinate species.

Conclusion

In conclusion, palladium nanoparticles stabilised by heteroatom donor-decorated polymer immobilised ionic liquids catalyse the Suzuki-Miyaura cross-coupling between aryl bromides and phenyl boronic acid with remarkable efficacy in aqueous media under exceptionally mild conditions. Catalyst stabilised by phosphino-decorated polymer immobilised ionic liquid (PdNP@PPh_2-PIILP) and its PEGylated counterpart (PdNP@PPh_2-PEGPIILP) were consistently more efficient than each of the other heteroatom donor-modified systems examined, across the range of substrates tested. Improvements in catalyst performance arising from the introduction of PEG are attributed to an increase in dispersibility and/or solubility facilitating access to more exposed active site. Catalysts generated *in-situ* from $PdCl_4$@PPh_2-PIILP or $PdCl_4$@PPh_2-PEGPIILP either compete with or outperform their *ex-situ* generated counterparts which offers numerous practical advantages for optimisation as well as substrate and reaction screening. The TONs obtained for the benchmark coupling are among the highest to be reported for PdNP-based catalysts in aqueous media under such mild conditions. As such, these results are highly encouraging and provide a strong platform to further study and explore the influence of the heteroatom donor on the nucleation and growth of nanoparticles and their

efficiency as catalysts. Moreover, the modular construction of the PIIL support will also enable properties such as surface characteristics, ionic microenvironment, heteroatom to metal ratio, hydrophilicity and porosity to be modified and thereby, ultimately, catalyst surface interactions, substrate accessibility and catalyst efficacy to be optimized.

Acknowledgements

We gratefully acknowledge Newcastle University for financial support (TB) and King Abdulaziz University, Saudi Arabia (Scholarship to H.F.A). Solid state ^{31}P and ^{13}C NMR spectra were obtained at the EPSRC UK National Solid State NMR Service at Durham University, high resolution mass spectra were obtained at the ESPRC National Mass Spectrometry Service in Swansea, XPS data was obtained at NEXUS the National EPSRC XPS Users Service at Newcastle University. FD-XAS was performed at BM28 at the ESRF (Experiment no. CH-5045) with help from Dr Laurence Bouchenoire and Dr Paul Thompson. We also thank Dr Maggie White for collecting the powder X-ray diffraction data (Newcastle) and Dr Kathryn White for the SEM images (Faculty of Medical Sciences, Newcastle University).

References

[1] a) C. C. C. Johansson, M. O. Seechurn, M. O. Kitching, T. J. Colacot, V. Sniekus, *Angew. Chem. Int. Ed.* **2012**, *51*, 5062–5085; b) B. A. Khakiani, K. Pourshamsian, H. Visi, *Appl. Organomet. Chem.* **2015**, *29*, 259–265; c) L. Ackermann, Modern Arylation Methods, Wiley-VCH, Weinheim, **2004**; d) N. Miyaura, A. Suzuki, *Chem. Rev.* **1995**, *95*, 2457–2483; e) A. Balanta, C. Godard, C. Claver, *Chem. Soc. Rev.* **2011**, *40*, 4973–4985; f) X. F. Wu, P. Anbarason, H. Neumann, M. Beller, *Angew. Chem. Int. Ed.* **2010**, *49*, 9047–9050; g) C. Torborg, M. Beller, *Adv. Synth. Catal.* **2009**, *351*, 3027–3043; h) J. Magano, J. R. Dunetz, *Chem. Rev.* **2011**, *111*, 2177–2250.

[2] For a selection of highly informative reviews see: a) C. A. Fleckenstein, H. Plenio, *Chem. Rev.* **2010**, *39*, 694–711; b) G. C. Fu, *Acc. Chem. Res.* **2008**, *41*, 1555–1564; c) D. S. Surry, S. L. Buchwald, *Angew. Chem. Int. Ed.* **2008**, *47*, 6338–6361; d) R. Martin, S. L. Buchwald, *Acc. Chem. Res.* **2008**, *41*, 1461–1473; e) D. S. Surry, S. L. Buchwald, *Chem. Sci.* **2011**, *2*, 27–50; f) F. Maiti, B. P. Fors, L. J. Henderson, Y. Nakamura, S. L. Buchwald, *Chem. Sci.* **2011**, *2*, 57–68; g) S. L. Buchwald, C. Mauger, G. Mignani, U. Scholz, *Adv. Synth. Catal.* **2006**, *348*, 23–39; h) A. Zapf, M. Beller, *Chem. Commun.* **2005**, 431–440; i) J. Magano, J. R. Dunetz, *Chem. Rev.* **2011**, *111*, 2177–2250; j) C. Torborg, M. Beller, *Adv. Synth. Catal.* **2009**, *351*, 3027–3043; k) N. C. Bruno, M. T. Tudge, S. L. Buchwald, *Chem. Sci.* **2013**, *4*, 916–920; l) A. Bruneau, M. Roche, M. Alami, S. Messaoudi, *ACS Catal.* **2015**, *5*, 1386–1396.

[3] a) A. Zapf, R. Jackstell, F. Rataboul, T. Riermeier, A. Monsees, C. Fuhrmann, N. Shaikh, U. Dingerdissen, M. Beller, *Chem. Commun.* **2004**, 38–39; b) S. Harkal, F. Rataboul, A. Zapf, C. Fuhrmann, T. Reirmeier, A. Monsees, M. Beller, *Adv. Synth. Catal.* **2004**, *346*, 1742–1748.

[4] a) R. J. Lundgren, B. D. Peters, P. G. Alsabeh, M. Stradiotto, *Angew. Chem. Int. Ed.* **2010**, *49*, 4071–4074; b) R. J. Lundgren, M. Stradiotto, *Angew. Chem. Int. Ed.* **2010**, *49*, 8686–8690; c) K. D. Hesp, R. J. Lundgre, M. Stradiotto, *J. Am. Chem. Soc.* **2011**, *133*, 5194–5197; d) R. J. Lundgren, A. Sappong-Kumankumah, M. Stradiotto, *Chem. Eur. J.* **2010**, *16*, 1983–1991; e) K. D. Hesp, M. Stradiotto, *J. Am. Chem. Soc.* **2010**, *132*, 18026–18029.

[5] a) S. Doherty, C. H. Smyth, J. G. Knight, A. S. K. Hashmi, *Nature Protocols* **2012**, *7*, 1870–1883; b) S. Doherty, C. H. Smyth, *Nature Protocols* **2012**, *7*, 1884–1896; c) S. Doherty, J. G. Knight, C. H. Smyth, G. A. Jorgensen, *Adv. Synth. Catal.* **2008**, *350*, 1801–1806; d) S. Doherty, J. G. Knight, J. P. McGrady, A. M. Ferguson, N. A. B. Ward, R. W. Harrington, W. Clegg, *Adv. Synth. Catal.* **2010**, *352*, 201–211; e) S. Doherty, J. G. Knight, N. A. B. Ward, D. M. Bittner, C. Wills, W. McFarlane, W. Clegg, R. W. Harrington, *Organometallics* **2013**, *32*, 1773–1788; f) S. Doherty, J. G. Knight, N. A. B. Ward, D. O. Perry, D. M. Bittner, M. R. Probert, S. A. Westcott, *Organometallics* **2014**, *33*, 5209–5219; g) A. S. K. Hashmi, A. Loos, A. Littmann, I. Braun, J. G. Knight, S. Doherty, F. Rominger, *Adv. Synth. Catal.* **2009**, *351*, 576–582; h) A. S. K. Hashmi, A. Loos, S. Doherty, J. G. Knight, K. J. Robson, F. Rominger, *Adv. Synth. Catal.* **2011**, *353*, 749–759; i) S. Doherty, J. G. Knight, C. H. Smyth, N. A. B. Ward, K. J. Robson, S. Tweedly, R. W. Harrington, W. Clegg, *Organometallics* **2010**, *29*, 4139–4157; j) S. Doherty, J. G. Knight, C. R. Addyman, C. H. Smyth, N. A. B. Ward, R. W. Harrington, *Organometallics* **2011**, *30*, 6010–6016.

[6] a) C. M. So, C. P. Lau, F. Y. Kwong, *Angew. Chem. Int. Ed.* **2008**, *47*, 8059–8063; b) C. M. So, C. C. Yeung, C. C. Lau, F. Y. Kwong, *J. Org. Chem.* **2008**, *73*, 7803–7806. c) C. M. So, C. P. Lau, A. S. C Chan, F. Y. Kwong, *J. Org. Chem.* **2008**, *73*, 7731–7734; d) C. M. So, Z. Zhou, C. P. Lau, F. Y. Kwong, *Angew. Chem. Int. Ed.* **2008**, *47*, 6402–6406; e) C. M. So, C. P. Lau, F. Y. Kwong, *Org. Lett.* **2007**, *9*, 2795–2798; f) C. M. So, H. W. Lee, C. P. Lau, F. Y. Kwong, *Org. Lett.* **2009**, *11*, 317–320; g) P. Y. Yeung, C. M. So, C. P. Lau, F. Y. Kwong, *Angew. Chem. Int. Ed.* **2010**, *49*, 8918–8922; h) P. Y. Yeung, K. H. Chung, F. Y. Kwong, *Org. Lett.* **2011**, *13*, 2912–2915.

[7] a) A. Bej, K. Ghosh, A. Sarkar, D. W. Knight, *RSC Adv.* **2016**, *6*, 11446–11453; b) M. Zahmakiran, S. Ozkar, *Nanoscale* **2011**, *3*, 3462–3481; c) A. Fihri, M. Bouhrara, B. Nekoueishahraki, J. M. Basset, V. Polshettiwar, *Chem. Soc. Rev.* **2011**, *40*, 4973–4985; d) M. Perez-Lorenzo, *J. Phys. Chem. Lett.* **2012**, *3*, 167–174.

[8] a) M. Turner, V. B. Golovko, O. P. H. Vaughan, P. Abdulkin, A. Berenguer-Murcia, M. S. Tikhov, B. F. G. Johnson, R. M. Lambert, *Nature* **2008**, *454*, 981–983; b) M. Stratakis, H. Garcia *Chem. Rev.* **2012**, *112*, 4469–4506; c) R. J. White, R. Luque, V. L. Budarin, J. H. Clark, D. J. Macquarrie, *Chem. Soc. Rev.* **2009**, *38*, 481–

494; d) Nanoparticles and Catalysis, Ed. D. Astruc, Wiley-VCH: New York, **2008**.
[9] a) H. Goesmann, C. Feldmann, *Angew. Chem. Int. Ed.* **2010**, *49*, 1362–1395. b) A. Roucoux, J. Schulz, H. Patin, *Chem. Rev.* **2002**, *102*, 3757–3778.
[10] a) X. F. Yang, A. Wang, B. Qiao, J. Li, J. Liu, T. Zhang, *Acc. Chem. Res.* **2013**, *46*, 1740–1748; b) G. Schmid, Nanoparticles: From Theory to Application, Wiley-VCH, Weinheim, **2004**, 1–359.
[11] a) D. Das, A. Sayari, *J. Catal.* **2007**, *246*, 60–65; b) M. Zhang, J. Guan, B. Zhang, D. Su, C. T. Williams, C. Liang, *Catal. Lett.* **2012**, 142, 313–318; c) O. Verho, K. P. J. Gustafson, A. Nagendiran, C.-W. Tai, J.-E. Bäckvall, *ChemCatChem* **2014**, *6*, 3153–3159; d) O. Verho, A. Nagendiran, C.-W. Tai, E. V. Johnston, J.-E. Bäckvall, *ChemCatChem* **2014**, *6*, 205–211; e) D. Sahu, A. R. Silva, P. Das, *Catal. Commun.* **2016**, *86*, 32–35; f) P. Gautam, M. Dihman, V. Polshettiwar, B. M. Bhange, *Green Chem.* **2016**, *18*, 5890–5899.
[12] a) A. Amali, R. Rana, *Green Chem.* **2009**, *11*, 1781–7186; b) A. Monopoli, A. Nacci, V. Calo, F. Ciminale, P. Cotugno, A. Mangone, L. C. Giannossa, P. Azzone, N. Cioffi, *Molecules* **2010**, *15*, 4511–4525; c) L. S. R. Lara, A. D. Zottis, W. C. Elias, D. Faggion Jr, C. E. Maduro de Campos, J. S. Acuña, J. B. Domingos, *RSC Adv.* **2015**, *5*, 8289–8296; d) M. Carrus, M. Fantauzzi, F. Riboni, M. Makosch, A. Rossi, E. Selli, J. A. van Bokhoven, *Appl. Catal. A* **2016**, *519*, 130–138; e) P. Wang, H. Zhu, M. Liu, J. Niu, B. Yuan, R. Li, J. Ma, *RSC Adv.* **2014**, *4*, 28922–28927.
[13] A. Corma, H. Garcia, A. Leyva, A. Primo, *Appl. Catal. A* **2003**, *247*, 41–49.
[14] a) M. Gómez-Martínez, E. Buxaderas, I. Pasto, D. Alonso, *J. Mol. Catal. A* **2015**, *404*, 1–7; b) D. V. Jawale, E. Gravel, C. Boudet, N. Shah, V. Geertsen, H. Li, I. N. N. Namboothiri, E. Doris, *Catal. Sci. Technol.* **2015**, *5*, 2388–2392; c) B. Cornelio, G. A. Rance, M. Laronze-Cochard, A. Fontana, J. Sapid, A. N. Khlobystov, *J. Mater. Chem. A* **2013**, *1*, 8737–8744; d) Z. Li, J. Liu, C. Xia, F. Li, *ACS Catal.* **2013**, *3*, 2440–2448; e) G. M. Scheuermann, L. Rumi, P. Steurer, W. Bannwarth, R. Mülhaupt, *J. Am. Chem. Soc.* **2009**, *131*, 8262–8270; f) Z. Li, J. Li, Z. Zhao, C. Xia, F. Li, *ChemCatChem* **2014**, *6*, 1333–1339; g) Y-.M. Lu, H.-Z. Zhu, W.-G. Li, B. Hu, S.-H. Yu, *J. Mater. Chem. A* **2013**, *1*, 3783–3788; h) F. Yang, A. Feng, C. Wang, S. Dong, C. Chi, X. Jia, L. Zhang, Y. Li, *RSC Adv.* **2016**, *6*, 16911–16916; i) E. Kim, H. S. Jeong, B. M. Kim, *Catal. Commun.* **2014**, *45*, 25–29; j) D. Nandi, S. Siwal, M. Choudhary, K. Mallick, *Appl. Catal. A* **2016**, *523*, 31–38; k) J. Sun, Y. Fu, G. He, X. Sun, X. Wang, *Catal. Sci. Technol.* **2014**, *4*, 1742–1748; l) Q. Fu, Y. Meng, Z. Fang, Q. Hu, L. Xu, W. Gao, X. Huang, Q. Xue, Y.-P. Sun, F. Lu, *ACS Appl. Mater. Interfaces* **2017**, *9*, 2469–2476.
[15] a) X. Li, Z. Guo, C. Xiao, T. W. Goh, D. Tesfagaber, W. Huang, *ACS Catal.* **2014**, *26*, 4056–4060; b) K. M. Choi, K. Na, G. A. Somorjai, O. M. Yaghi, *J. Am. Chem. Soc.* 2**015**, 137, 3490–3497; c) P. Hu, J. V. Morabito, C.-K. Tsung, *ACS Catal.* **2014**, *4*, 4409–4419; d) Y.-Z. Chen, Q. Xu, S.-H. Yu, H.-L. Huang, *Small* **2015**, *11*, 71–76; e) G. Huang, Q. Yang, Q. Xu, S.-H. Yu, H.-L. Jiang, *Angew. Chem. Int. Ed.* **2016**, *55*, 7379–7383; f) D. Sun, Z. Li, *J. Phys. Chem. C* **2016**, *120*, 19744–19750; g) Y. Huang, Z. Zheng, T. Liu, J. Lü, Z. Lin, H. Li, R. Cao, *Catal. Commun.* **2011**, *14*, 27–31; h) T. T. Dang, Y. Zhu, J. S. Y. Ngiam, S. C. Ghosh, A. Chen, A. M. Seayad, *ACS Catal.* **2013**, *3*, 1406–1410.
[16] a) C. Marrodan, D. Berti, F. Liguori, P. Barbaro, *Catal. Sci. Technol.* **2012**, *2*, 2279–2290; b) F. Liguori, P. Barbaro, *J. Catal.* **2014**, *311*, 212–220; c) M. M. Dell'Anna, M. Mali, P. Mastrorilli, A. Rizzuti, C. Ponzoni, C. Leonelli, *J. Mol. Catal. A* **2013**, *366*, 186–194; d) Y. Yang, S. Ogasawara, G. Li, S. Kato, *J. Mater. Chem.* **2013**, *1*, 3700–3705; e) C. Deraedt, L. Salmon, J. Ruiz, D. Astruc , *Adv. Synth. Catal.* **2013**, *355*, 2992–3001; f) G. Hahn, J.-K Ewert, C. Denner, D. Tilgner, R. Kempe, *ChemCatChem* **2016**, *8*, 2461–2465; g) P. M. Uberman, C. S. García, J. R. Rodriguez, S. E. Martin, *Green Chem.* **2017**, *19*, 739–748.
[17] For recent informative reviews see: a) J. Dupont, *Acc. Chem. Res.* **2011**, *44*, 1223–1231; b) P. Wasserscheid, T. Welton, *Ionic Liquids in Synthesis*, Wiley-VCH, Weinheim, 2007; c) S. Doherty in *Catalysis in Ionic Liquids*: *From Catalyst Synthesis to Applications*, Eds. C. Hardacre, V. Parvulescu, RSC Catalysis Series, The Royal Society of Chemistry, **2014**, pp 44–308.
[18] a) X. Mu, D. G. Evans, K. Kou, *Catal. Lett.* **2004**, *97*, 151–154; b) A. Papp, K. Miklós, P. Forgo, A. Molnár, *J. Mol. Catal. A* **2005**, *229*, 107–116; c) M. Besson, P. Gallezot, *Catal. Today* **2003**, *81*, 547–559.
[19] a) A. P. Umpierre, P. F. P. Fichtner, S. R. Teixeira, J. Dupont, *Chem. Eur. J.* **2003**, *9*, 3263–3269; b) F. Bellina, C. Chiappe, *Molecules* **2010**, *15*, 2211–2245; Y. Liu, S.-S. Wang, W, Liu, Q.-X. Wan, H.-H. Wu, G. H. Gao, *Curr. Org. Chem.* **2009**, *13*, 1322–1346.
[20] a) A. Zhang, H. Cui, *Langmuir* **2009**, *25*, 2604–2612; b) Z. Wang, Q. Zhang, D. Kuehner, A. Ivaska, L. Niu, *Green Chem.* **2008**, *10*, 907–909.
[21] a) B. C. Leal, C. S. Consorti, G. Machado, J. Dupont, *Catal. Sci. Technol.* **2015**, *5*, 903–909; b) K. L. Luska, A. Moores, *Adv. Synth. Catal.* **2011**, *353*, 3167–3177; c) S. A. Straton, K. L. Luska, A. Moores, *Catal. Today* **2012**, *183*, 96–100; d) K. L. Luska, K. Z. Demmans, S. A. Stratton, A. Moores, *Dalton Trans.* 2011, **2012**, 41, 13533–13540.
[22] a) D. B. Zhao, Z. F. Fei, T. J. Geldbach, R. Scopelliti,, P. J. Dyson, *J. Am. Chem. Soc.* **2004**, *126*, 15876–15882; b) C. Chiappe, D. Pieraccini, D. Zhao, Z. Fei, P. J. Dyson, *Adv. Synth. Catal.* **2006**, *348*, 68–74; c) Z. Fei, D. Zhao, D. Pieraccini, W. H. Ang, T. J. Geldbach, R. Scopelliti, C. Chiappe, P. J. Dyson, *Organometallics* **2007**, *26*, 1588–1598; d) X. Yang, Z. Fei, D. Zhao, W. H. Ang, Y. Li, P. J. Dyson, *Inorg. Chem.* **2008**, *47*, 3292–3297; e) M. H. G. Prechtl, J. D.; Scholten, J. Dupont, *J. Mol. Catal. A* **2009**, *313*, 74–78.
[23] a) H. Itoh, K. Maka, Y. Chujo, *J. Am. Chem. Soc.* **2004**, *126*, 3026–3027; b) N. Kocharova, J. Leiro, J. Lukkari, M. Heinonen, T. Skala, F. Sutara, M. Skoda, M. Vondracek, *Langmuir* **2008**, *24*, 3235–3242.
[24] a) Konnerth, M. H. G. Prechtl, *Green Chem.* **2017**, *19*, 2762–2767; b) N. Yan, X. Yang, Z. Fei, Y. Li, Y. Kou, P. J. Dyson, *Organometallics* **2009**, *28*, 937–939; c) X.

Yuan, N. Yan, S. A. Katsyuba, E. E. Svereva, Y. Kou, P. J. Dyson, *Phys. Chem. Chem. Phys.* **2012**, *14*, 6026–6033.

[25] a) B. Léger, A. Denicourt-Nowicki, A. Roucoux, H. Olivier-Bourbigou, *Adv. Synth. Catal.* **2008**, *350*, 153–159; b) B. Léger, A. Denicourt-Nowicki, H. Olivier-Bourbigou, A. Roucoux, *Inorg. Chem.* **2007**, *47*, 9090–9096; c) A. Denicourt-Nowicki, B. Léger, A. Roucoux, *Phys. Chem. Chem. Phys.* **2011**, *13*, 13510–13517; d) R. R. Dykeman, N. Yan, R. Scopelliti, P. J. Dyson, *Inorg. Chem.* **2011**, *50*, 717–719.

[26] K. L. Luska, A. Moores, *ChemCatChem* **2012**, *4*, 1534–1546.

[27] a) B. C. Leal, C. S. Consorti, G. Machado, J. Dupont, *Catal. Sci. Technol.* **2015**, *5*, 903–909; b) Z. Wu, H. Jiang, *RSC Adv.* **2015**, *5*, 34622–34629; c) Y. Hu, Y. Y. Yu, Z. S. Hou, H. Li, X. G. Zhao, B. Feng. *Adv. Synth. Catal.* **2008**, *350*, 2077–2085.

[28] Y. Hu, Y. Y. Yu, Z. S. Hou, H. M. Yang, B, Feng, H. Li, Y. X. Qiao, X. R. Wang, L. Hua, Z. Y. Pan, X. Zhao. *Chem. Asian J.* **2010**, *5*, 1178–1184.

[29] a) H. Jiang, X. Zheng, *Catal. Sci. Technol.* **2015**, *5*, 3728–3734. b) H. Jiang, X. Zheng, *Appl. Catal. A* **2015**, *499*, 118–123.

[30] For highly insightful and informative reviews on polyionic liquids and applications see: a) F. Giacalone, M. Gruttadauria, *ChemCatChem* **2016**, 8, 664–684; b) J. Lu, F. Yan, J. Texter, *Prog. Polym. Sci.* **2009**, *34*, 431–448; c) J. Yuan, D. Mecerreyes, M. Antonietti, *Prog. Polym. Sci.* **2013**, *38*, 1009–1036; d) D. Mecerreyes, *Prog. Polym. Sci.* **2011**, *36*, 1629–1648; d) O. Green, S. Grubjesic, S. Lee, M. A. Firestone, *Polym. Rev.* **2009**, *49*, 339–360; e) H. Li, P. S. Bhadury, B. Song, S. Yang, *RSC Adv.* 2012, 2, 12525–12551; f) J. Yuan, M. Antonietti, *Polymer* 2**011**, 52, 1469–1482; g) T. K. Carlisle, J. E. Bara, A. L. Lafrate, D. L. Gin, R. D. Noble, *J. Membr. Sci.* **2010**, *359*, 37–43.

[31] a) B. Van Vaerenbergh, J. Lauwaert, W. Bert, J. W. Thybaut, J. De Clercq, P. Wermeir, *ChemCatChem* **2017**, *9*, 451–457; b) M. I. Burguete, E. García-Verdugo, I. Garcia-Villar, F. Gelat, P. Licence, S. V. Luis, V. Sans, *J. Catal.* **2010**, *269*, 150–160; c) G. Liu, M. Hou, J. Song, T. Jiang, H. Fan, Z. Zhang, B. Han, *Green Chem.* **2010**, *12*, 65–69; d) S. Li, J. Wang, Y. Kou, S. Zhang, *Chem. Eur. J.* **2010**, *16*, 1812–1818; e) H. Zhao, Y. Wang, R. Wang, *Chem. Commun.* **2014**, *50*, 10871–10874; f) Y. Wang, H. Zhong, L. Li, R. Wang, *ChemCatChem* **2016**, *8*, 2234–2240; g) Y. Su, X. li, Y. Wang, H. Zhong, R. Wang, *Dalton Trans.* **2016**, *45*, 16896–16903; h) N. Jiao, Z. Li, Y. Wang, J. Liu, C. Xia, *RSC Adv.* **2015**, *5*, 26913–26922.

[32] a) S. Doherty, J. G. Knight, T. Backhouse, E. Abood, H. Alshaikh, I. J. S. Fairlamb, R. A. Bourne, T. W. Chamberlain, R. Stones, *Green Chem.* **2017**, *19*, 1635–1641; b) S. Doherty, J. G. Knight, T. Backhouse, A. Bradford, F. Saunders, R. A Bourne, T. W. Chamberlain, R. Stones, A. Clayton, K. Lovelock, *Catal. Sci. Technol.* **2018**, *8*, 1454–1467.

[33] J. Tan, J. Cui, G. Ding, T. Deng, Y. Zhu, Y.-w. Li, *Catal. Sci. Technol.* **2016**, *6*, 1469–1475.

[34] S. Jayakumar, A. Modak, M. Guo, H. Li, X. Hu, Q. Yang, *Chem. Eur. J.* **2017**, *23*, 7791–7797.

[35] a) J. L. Castelbou, A. Gual, E. Mercadé, C. Claver, C. Godard, *Catal. Sci. Technol.* **2013**, *3*, 2828–2833; b) D. González-Gálvez, P. Nolis, K. Philippot, B. Chaudret, P. W. N. M. van Leeuwen, *ACS Catal.* **2012**, *2*, 317–321; c) D. González-Gálvez, P. Lara, O. Rivada-Wheelaghan, S. Conejero, B. Chaudret, K. Philippot, P. W. N. M. van Leeuwen, *Catal. Sci. Technol.* **2013**, *3*, 99–105; d) J. L. Castelbou, E. Bresó-Femenia, P. Blondeau, B. Chaudret, S. Castillón, C. Claver, C. Godard, *ChemCatChem* **2014**, *6*, 3160–3168. e) I. Cano, A. M. Chapman, A. Urakawa, P. W. N. M. van Leewuen, *J. Am. Chem. Soc.* **2014**, *136*, 2520–2538.

[36] a) L. M. Martínez-Prieto, A. Ferry, L. Rakers, C. Richter, P. Lecante, K. Philippot, B. Chaudret, F. Glorius, *Chem. Commun.* **2016**, *52*, 4768–5771; b) C. Richter, K. Schaepe, F. Glorius, B. J. Ravoo, *Chem. Commun.* **2014**, *50*, 3204–3207; c) P. Lara, L. M. Martinez-Prieto, M. Rosello-erino, C. Richter, F. Glorius, S. Conejero, K. Philippot, B. Chaudret, *Nano-Struct. Nano-Objects* **2016**, *6*, 39–45; d) A. Rühling, K. Schapep, L. Rakers, B. Vonhören, P. Tegeder, B. J. Ravoo, F. Glorius, *Angew. Chem. Int. Ed.* **2016**, *55*, 5856–5860; e) A. Ferry, K. Schaepe, P. Tegeder, C. Richter, K. M. Chepiga, B. J. Ravoo, F. Glorius, *ACS Catal.* **2015**, *5*, 5414–5420.

[37] J. B. Ernst, C. Schwermann, G. Yokota, M. Tada, S. Muratsugu, N. L. Doltsinis, F. Glorius, *J. Am. Chem. Soc.* **2017**, *139*, 9144–9147.

[38] J. B. Ernst, S. Muratsugu, F. Wang, M. Tada, F. Glorius, *J. Am. Chem. Soc.* **2016**, *138*, 10718–10721.

[39] a) Y. Borodko, S. E. Habas, M. Koebel, P. D. Yang, H. Frei, G. A. Somorjai, *J. Phys. Chem. B.* **2006**, *110*, 23052–23059; b) Y. Borodko, H. S. Lee, S. H. Joo, Y. Zhang, G. A. Somorjai, *Phys. Chem. C* **2010**, *114*, 1117–1126.

[40] a) J.-K. Sun, Z. Kochovski, W.-Y. Zhang, H. Kirmse, Y. Lu, M. Antonietti, J. Yuan, *J. Am. Chem. Soc.* **2017**, *139*, 8971–8976; b) K. Chen, H. Wu, Q. Hua, S. Chang, W. Huang, *Phys. Chem. Chem. Phys.* **2013**, *15*, 2272–2277. For a selection of additional relevant examples see: c) H. Tsunoyama, N. Ichikuni, H. Sakurai, T. Tsukuda, *J. Am. Chem. Soc.* **2009**, *131*, 7086–7093; d) B. Feng, Z. Hou, H. Yang, X. Wang, Y. Hu, H. Li, Y. Qiao, X. Zhao, Q. Huang, *Langmuir* **2010**, *26*, 2505–2513; e) E. Gross, J. H.-C. Liu, F. D. Toste, G. A. Somorjai, *Nat. Chem.* **2012**, *4*, 94952; f) S. T. Marshall, M. O'Brien, B. Oetter, A. Corpuz, R. M. Richards, D. K. Schwartz, J. W. Medlin, *Nat. Mater.* **2010**, *9*, 853–958; g) J. Xian, Q. Hua, Z. Jiang, Y. Ma, W. Huang, *Langmuir* **2012**, *28*, 6736–6741.

[41] a) G. H. Jeong, S. H. Kim, M. Kim, D. Choi, J. H. Lee, J.-H. Kim, S.-W Kim, *Chem. Commun.* **2011**, *47*, 12236–12238; b) W. Zhu, H. Yang, Y. Yu, L. Hua, H. Li, B. Feng, Z. Hou, *Phys. Chem. Chem. Phys.* **2011**, *13*, 13492–13500; c) J. Sun, Y. Fu, G. He, X. Sun, X. Wang, *Catal. Sci. Technol.* **2014**, *4*, 1742–1748.

[42] a) Z. Li, J. Li, Z. Zhao, C. Xia, F. Li, *ChemCatChem* **2014**, *6*, 1333–1339; b) Z. Zhang, F. Wang, C. Chen, T. Zhang, X. Jiang, Z. Yun, *RSC Adv.* **2014**, *4*, 45088–45094.

[43] a) N. J. S. Costa, P. K. Kiyohara, A. L. Montiero, Y. Coppel, K. Philippot, L. M. Rossi, *J. Catal.* **2010**, *276*, 382–389; b) L. M. Rossi, I. M. Nangoi, N. J. S. Costa, *Inorg. Chem.* **2009**, *48*, 4640–4642; c) D. Zhang, Y. Guan, E. J. M. Hensen, T. Xue, Y. Wang, *Catal. Sci. Technol.* **2014**, *4*, 795–802; d) E. Rafter, T. Gutmann, F. Löw, G. Buntkowsky, K. Philippot, B. Chaudret,, P. W. N. M. van Leeuwen, *Catal. Sci. Technol.* **2013**, *3*, 595–599; e) G. Salas, C. C. Santini, K. Phillippot, V. Colliere, B. Chaudret, B. Fenet, P. F. Fazzini, *Dalton Trans.* **2011**, *40*, 4660–4666.
[44] C. Wang, R. Ciganda, L. Salmon, D. Gregurec, J. Irigoyen, S. Moya, J. Ruiz, D. Astruc, *Angew. Chem. Int. Ed.* **2016**, *55*, 3091–3095.
[45] X. Liu, X. Zhao, M. Lu, *Appl. Organomet. Chem.* **2015**, *29*, 419–424.
[46] N. Mejías, R. Pleixats, A. Shafir, M. Medio-Simón, G. Asensio, *Eur. J. Org. Chem.* **2010**, 5090–5099.
[47] X. Liu, X. Zhao, M. Lu, *Catal. Lett.* **2015**, *145*, 1549–1556.
[48] S–W. Kim, S. Kim, J. B. Tracy, A. Jasanoff, M. G. Bawendi, *J. Am. Chem. Soc.* **2005**, *127*, 4556–4557.
[49] N. Mejías, A. Serra-Muns, R. Pleixats, A. Shafir, M. Tristany, *Dalton Trans.* **2009**, 7748–7755.
[50] S. Bahadorikhalili, L. Ma'mani, H. Mahdavi, A. Shafiee, *RSC Adv.* **2015**, *5*, 71297–71305.
[51] S. Sawoo, D. Srimani, P. Dutta, R. Lahiri, A. Sarkar, *Tetrahedron* **2009**, *65*, 4367–4374.
[52] S. Lou, G. C. Fu, *Adv. Synth. Catal.* **2010**, *352*, 2081–2084.
[53] Yafei Guo, Jiuling Li, Xiwei Shi, Yang Liu, Kai Xie, Yuqi Liu, Yubo Jiang, Bo Yang, Rui Yang, *Appl. Organomet. Chem.* DOI.org/10.1002/aoc.3592.
[54] M. Planellas, R. Pleixats, A. Shafir, *Adv. Synth. Catal.* **2012**, *354*, 651–662.
[55] B. Karimi, D. Elhamifar, J. H. Clark, A. J. Hunt, *Chem. Eur. J.* **2010**, *16*, 847–8053.
[56] A. Dewan, P. Bharali, U. Bora, A. J. Thakur, *RSC Adv.* **2016**, *6*, 11758–11762.
[57] L. A. Bivona, F. Giacalone, L. Vaccaro, C. Aprile, M. Gruttadauria, *ChemCatChem* **2015**, *7*, 2526–2533.
[58] a) M. Gruttadauria, L. F. Liotta, A. M. P. Salvo, F. Giacalone, V. La Parola, C. Aprile, R. Noto, *Adv. Synth. Catal.* **2011**, *353*, 2119–2130; b) C. Pavia, E. Ballerini, L. A. Bivona, F. Giacalone, C. Aprile, L. Vaccaro, M. Gruttadauria, *Adv. Synth. Catal.* **2013**, 355, 2007–2018.
[59] G. Ding, W. Wang, T. Jiang, B. Hu, *Green Chem.* **2013**, *15*, 3396–3403.
[60] D. Peral, F. Gómez-Villarraga, X. Sala, J. Pons, J. C. Bayón, J. Ros, M. Guerrero, L. Vendier, P. Lecante, J. García-Antón, K. Philippot, *Catal. Sci. Technol.* **2013**, *3*, 475–489.
[61] R. B. Boysen, R. K. Szilagyi, *Inorg. Chim. Acta* **2008**, *361*, 1047–1058.
[62] For insightful and informative reviews see: a) A. Bej, K. Ghosh, A. Sarka, D. W. Knight, *RSC Adv.* **2016**, *6*, 11446–11453; b) N. T. S. Phan, M. Van Der Sluys, C. W. Jones, *Adv. Synth. Catal.* **2006**, *348*, 609–679.
[63] A. F. Lee, P. J. Ellis, I. J. S. Fairlamb, K. Wilson, *Dalton Trans.* **2010**, *39*, 10473–10482.
[64] a) G. M. Whitesides, M. Hackett, R. L. Brainard, J.-P. P. M. Lavalleye, A. F. Sowinski, A. N. Izumi, S. S. Moore, D. W. Brown, E. M. Staudt, *Organometallics* **1985**, *4*, 1819–1830; b) K. Q. Yu, W. Sommer, J. M. Richardson, W. Weck, C. W. Jones, *Adv. Synth. Catal.* **2005**, *347*, 161–171.
[65] N. T. S. Phan, M. V. Sluys, C. W. Jones, *Adv. Synth. Catal.* **2006**, *348*, 609–616.

